Microinfarct disruption of white matter structure

A longitudinal diffusion tensor analysis

Eitan Auriel, MD, MSc
Brian L. Edlow, MD
Yael D. Reijmer, PhD
Panagiotis Fotiadis, BSc
Sergi Ramirez-Martinez, MD
Jun Ni, MD
Anne K. Reed, BA
Anastasia Vashkevich, BA
Kristin Schwab, BA
Jonathan Rosand, MD, MSc
Anand Viswanathan, MD, PhD
Ona Wu, PhD
M. Edip Gurol, MD, MSc
Steven M. Greenberg, MD, PhD

Correspondence to Dr. Greenberg: sgreenberg@partners.org

ABSTRACT

Objective: To evaluate the local effect of small asymptomatic infarctions detected by diffusion-weighted imaging (DWI) on white matter microstructure using longitudinal structural and diffusion tensor imaging (DTI).

Methods: Nine acute to subacute DWI lesions were identified in 6 subjects with probable cerebral amyloid angiopathy who had undergone high-resolution MRI both before and after DWI lesion detection. Regions of interest (ROIs) corresponding to the site of the DWI lesion (lesion ROI) and corresponding site in the nonlesioned contralateral hemisphere (control ROI) were coregistered to the pre- and postlesional scans. DTI tractography was additionally performed to reconstruct the white matter tracts containing the ROIs. DTI parameters (fractional anisotropy [FA], mean diffusivity [MD]) were quantified within each ROI, the 6-mm lesion-containing tract segments, and the entire lesion-containing tract bundle. Lesion/control FA and MD ratios were compared across time points.

Results: The postlesional scans (performed a mean 7.1 ± 4.7 months after DWI lesion detection) demonstrated a decrease in median FA lesion/control ROI ratio (1.08 to 0.93, $p = 0.038$) and increase in median MD lesion/control ROI ratio (0.97 to 1.17, $p = 0.015$) relative to the prelesional scans. There were no visible changes on postlesional high-resolution T1-weighted and fluid-attenuated inversion recovery images in 4 of 9 lesion ROIs and small (2–5 mm) T1 hypointensities in the remaining 5. No postlesional changes in FA or MD ratios were detected in the 6-mm lesion-containing tract segments or full tract bundles.

Conclusions: Asymptomatic DWI lesions produce chronic local microstructural injury. The cumulative effects of these widely distributed lesions may directly contribute to small-vessel–related vascular cognitive impairment. *Neurology*® 2014;83:182–188

GLOSSARY

CAA = cerebral amyloid angiopathy; **CMI** = cerebral microinfarct; **DTI** = diffusion tensor imaging; **DWI** = diffusion-weighted imaging; **FA** = fractional anisotropy; **FLAIR** = fluid-attenuated inversion recovery; **MD** = mean diffusivity; **MEMPRAGE** = multiecho magnetization-prepared rapid-acquisition gradient echo; **MNI** = Montreal Neurological Institute; **ROI** = region of interest.

Cerebral microinfarcts (CMIs) appear to be the single most widespread type of brain infarction.[1] Although the total number of CMIs is difficult to determine, mathematical modeling suggests they typically range in the hundreds or thousands.[2] These numbers suggest that CMIs may substantially affect neurologic function, a possibility supported by clinical-pathologic studies.[3–6] It remains unclear, however, whether such tiny lesions (typically <1-mm diameter[1]) are capable of disrupting brain structure.

A prerequisite for analyzing the effect of CMIs is the ability to detect them in vivo. Two MRI approaches have been advanced to detect CMIs: high-field-strength structural imaging[7,8] and diffusion-weighted imaging (DWI), which demonstrates restricted diffusion approximately 1 to 2 weeks poststroke.[9,10] This narrow temporal window substantially limits lesion detectability, but has the virtue of providing information about lesion timing, making it possible to compare tissue structure before and after CMI occurrence.

Supplemental data at Neurology.org

From the J. Philip Kistler Stroke Research Center, Department of Neurology, Massachusetts General Hospital and Harvard Medical School, Boston, MA.

Go to Neurology.org for full disclosures. Funding information and disclosures deemed relevant by the authors, if any, are provided at the end of the article.

We examined whether small DWI lesions cause structural changes detectable on postlesional follow-up imaging. To do so, we took advantage of the unique opportunity provided by our ongoing serial high-resolution MRI study of patients with cerebral amyloid angiopathy (CAA), a small-vessel disease associated with relatively frequent DWI lesions.[11–13] Postlesional changes were assessed by measuring alterations in magnitude and directionality of water diffusion with diffusion tensor imaging (DTI)[14,15] as well as by high-resolution T1- and T2-weighted MRI. To determine the extent of the lesions' structural impact, we analyzed both the lesions themselves and their surrounding fiber tracts.

METHODS

Study population. Study subjects were identified from a prospective cohort of patients with CAA who underwent serial MRI scans to assess the natural history of the disease.[16] The diagnosis of probable or definite CAA was based on the Boston Criteria.[17] Detailed information, including demographics, vascular risk factors, and characteristics of the presenting event, was prospectively recorded at the time of cohort entry. All subjects routinely underwent MRI scans including T1-weighted multiecho magnetization-prepared rapid-acquisition gradient echo (MEMPRAGE), T2-weighted fluid-attenuated inversion recovery (FLAIR) and diffusion imaging, which includes both DWI and DTI data acquisition. In 2011 to 2013, all study participants with a prior "prelesional" research-protocol MRI were prospectively recruited to undergo up to 5 research DWI scans over 2 years, which were reviewed in real time for the occurrence of DWI hyperintense lesions. Subjects with an identified DWI lesion in the white matter (defined as the "lesional" scan) were then prospectively scheduled for a "postlesional" follow-up research-protocol MRI. The postlesional MRI in one subject (subject C in the table) showed a new DWI lesion, and the subject was accordingly offered one further postlesional research-protocol study.

Standard protocol approvals, registrations, and patient consents. Study procedures were approved by the hospital institutional review board, and all participants provided informed written consent.

Image acquisition and lesion identification. All subjects underwent MRI examination of the brain on a 1.5-tesla Signa scanner (GE Medical Systems, Milwaukee, WI). DWIs and DTIs were obtained using a single-shot spin-echo, echo-planar imaging sequence with the following parameters: repetition time/echo time 8,270/82 milliseconds, voxel size 2 mm (isotropic), acquisition matrix 128 × 128 × 64; 60 isotropically distributed diffusion-sensitizing gradients with a b value = 700 s/mm^2, and 10 b = 0 s/mm^2 (b0). High-resolution FLAIR and MEMPRAGE images were obtained using methods previously reported[13,16] with voxel size 1 mm (isotropic). All DWI scans were reviewed for the presence of lesions by a clinical neurologist (E.A.) and confirmed by a vascular neurologist (M.E.G.), using criteria previously described and demonstrated to have high interrater reliability.[13] After identifying a DWI lesion, the T1-weighted MEMPRAGE and T2-weighted FLAIR sequences on the postlesional scan were reviewed for any abnormal signal at the corresponding neuroanatomical coordinates using coregistration techniques (see below). One subject (subject A) did not have a FLAIR sequence on the postlesional scan.

Image processing. We created a control region of interest (ROI) in the contralateral hemisphere for comparison to each DWI lesion, using a multistep coregistration procedure (see full details in e-Methods and figure e-1 on the *Neurology*® Web site at Neurology.org). Briefly, we applied nonlinear transformation from each subject's native b0 space to a common Montreal Neurological Institute (MNI) space via native T1 space, using tools from the FMRIB Software Library (FSL),[18] to create a transformation warp-field for the whole brain volume. This warp-field was used to coregister the DWI lesions to MNI space. A control ROI was then generated using the same neuroanatomical coordinates in the contralateral hemisphere in MNI space. Finally, the control ROI was transformed back into native b0 space using the inverse of the nonlinear warp-field. Precise localization of the control ROIs in native b0 space was verified by comparing the location of the lesion ROI and the control ROI on the color-coded fiber orientation maps using a standard color atlas[19] with manual adjustment as necessary and without reference to quantitative fractional anisotropy (FA) or mean diffusivity (MD) data to minimize bias. The lesion and control ROIs were then transformed to the prelesional and postlesional b0 native space datasets using a similar nonlinear coregistration process. Each b0 dataset is inherently coregistered to the DWI and DTI volumes, enabling quantitative analysis of diffusion parameters within lesion and control ROIs at each time point.

Diffusion tractography was performed by constrained spherical deconvolution.[20] Individual fiber bundles were delineated

Table Subjects with a DWI lesion and pre- and postlesional scans

Subject	Age at lesion detection, y	Prelesional to postlesional interscan interval, mo	No. of DWI lesions	DWI lesion location (white matter bundle)
A	68	19.9	1	Cingulum bundle
B	58	24	1	Middle longitudinal fasciculus[30]
C 1	69	12	3	Inferior frontal gyrus U fibers, cerebellar hemisphere (2 lesions)
C 2	69	12	1	Cerebellar hemisphere
D	73	12.5	1	Middle longitudinal fasciculus
E	56	23.7	1	Corpus callosum
F	79	14.2	1	Angular gyrus U fibers

Abbreviation: DWI = diffusion-weighted imaging.

Figure 1 Representative ROIs for analysis

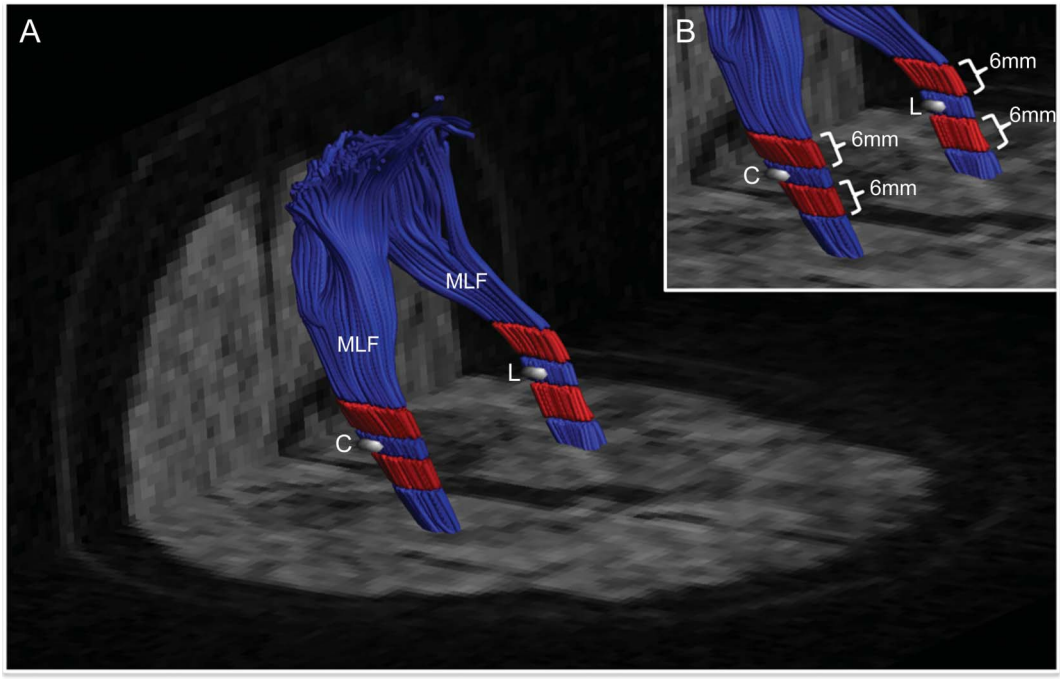

(A, B) Reconstruction of the MLF tract containing the DWI lesion (L) and the corresponding contralateral control ROI (C) at the time of lesion detection in subject B. FA and MD were measured within the lesion and control ROIs (white), the 6-mm segments surrounding the ROIs (red), and along the full bundles (red plus blue). DWI = diffusion-weighted imaging; FA = fractional anisotropy; MD = mean diffusivity; MLF = middle longitudinal fasciculus; ROI = region of interest.

from the whole-brain tractography maps using an ROI-based approach (see e-Methods for details). Diffusion properties (FA and MD) were investigated within each ROI, within a 6-mm segment along the fiber bundle on each side of the ROI (figure 1, red tracts) and along the entire fiber bundle (figure 1, red plus blue tracts). All ROI determination and tractography were performed on the color-coded fiber orientation maps without access to the quantitative FA and MD maps.

All cases were included in the longitudinal analysis of FA and MD within the lesion and control ROIs. Two lesions were excluded from the fiber tractography analysis: one (subject A) because of a large hemorrhage within the control fiber bundle and different DTI acquisition parameters (i.e., 30 diffusion-encoding directions) on the follow-up scan, and the second (subject C, inferior frontal U-fiber lesion) because of inability to reliably reconstruct the tracts. In total, 9 lesions from 6 subjects were included in the ROI analysis and 7 lesions from 5 subjects were included in the tractography analysis. To minimize the effect of interscan variability as well as potential diffuse effects of progressive aging and small-vessel disease, we performed all longitudinal comparisons using the ratio of lesion-to-control FA and MD values for the ROIs, short-segment tracts, and full bundle of tracts as suggested by a previous report.[21]

Statistical analysis. Our prespecified primary hypothesis was that incident DWI lesions would result in focally decreased FA and increased MD ratios within the lesion ROIs on postlesional relative to prelesional scans. Changes within the 6-mm segments surrounding the ROIs and within the whole fiber bundles (figure 1) were evaluated as exploratory secondary analyses. Comparisons of median FA and MD ratios were performed using Wilcoxon paired signed-rank test, and comparisons of pre- to postlesional change in FA and MD using paired t test. A threshold of $p < 0.05$ was used for significance.

RESULTS Six subjects (table; mean age 67 ± 9 years) had a total of 9 DWI lesions; 5 of the 6 had a single DWI lesion, while one (subject C) had 3 lesions on one scan and a fourth on a consecutive scan. By design, all subjects had high-resolution structural MRI and DTI performed prior and subsequent to the appearance of the DWI lesions. The mean time interval between the prelesional and postlesional scans was 16.9 ± 5.5 months and between the lesion-detecting DWI and the postlesional scans was 7.1 ± 4.7 months. Eight of the 9 lesions were judged to be acute based on hypointense signal on the corresponding diffusivity map, and the remaining lesion was judged to be subacute based on isointense diffusivity.

Structural T1-weighted and FLAIR imaging. Comparison of pre- and postlesional high-resolution T1-weighted and FLAIR images revealed no visible signal changes at the sites of 4 of the 9 DWI lesions. Two of the remaining 5 DWI lesions were associated with appearance on the postlesional scans of very small (approximately 2 mm in largest diameter) foci of T1 hypointensity (figure 2A): one with associated FLAIR hyperintensity; the other without. The other 3 DWI lesions were associated with appearance of somewhat larger (approximately 5–6 mm in largest diameter;

Figure 2 Structural lesions on postlesional MRI

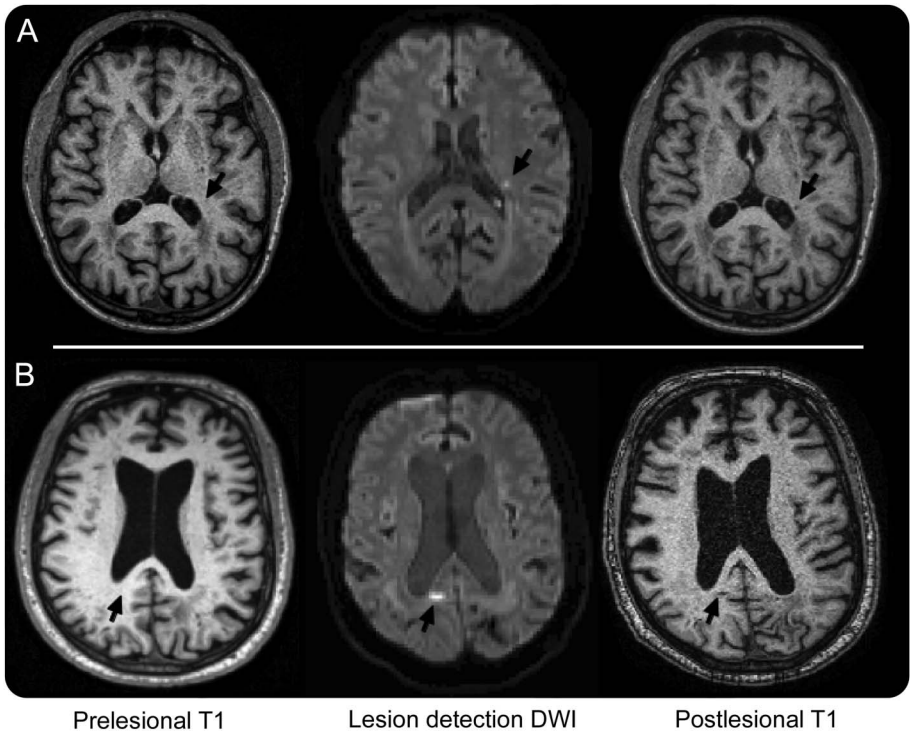

A set of prelesional T1-weighted MEMPRAGE, lesion-detection DWI, and postlesional T1-weighted MEMPRAGE images are shown for subjects D (A) and A (B), with the corresponding lesion sites indicated by arrows. The DWI lesions shown are 2 of the 5 with visible postlesional T1 changes. DWI = diffusion-weighted imaging; MEMPRAGE = multiecho magnetization-prepared rapid-acquisition gradient echo.

figure 2B) foci of T1 hypointensity and FLAIR hyperintensity, throughout the lesion or in a rim around a FLAIR hypointense center.

ROI-based DTI analysis. Quantitative analysis of DTI measures at the location of the DWI lesions demonstrated decreased FA and increased MD at the time of the postlesional MRI. The median FA lesion/control ratio within the ROI decreased on the postlesional images from 1.08 to 0.93 ($p = 0.038$) and the median MD ratio increased from 0.97 to 1.17 ($p = 0.015$) relative to the prelesional images. There were no differences between DWI lesions with postlesional T1 or FLAIR abnormalities relative to those without in pre- to postlesional change in FA or MD ratio (figure 3; $p = 0.15$ for change in FA ratio, $p = 0.40$ for MD ratio). There were also no associations between change in FA or MD ratio and subject age, side of lesion (left vs right), or interscan interval. At the time of lesion detection, the median FA ratio decreased from 1.08 to 0.68 ($p = 0.015$) and median MD ratio decreased from 0.97 to 0.89 ($p = 0.086$) relative to the prelesional ratios.

Tract-based DTI analysis. For the 7 DWI lesions in which fiber tractography could be performed, effects of the DWI lesions were not demonstrated in the surrounding 6-mm fiber segments or encompassing fiber tracts. Within the short segment of fiber tracts, there was no detectable change in median FA ratio (0.98 prelesional vs 0.81 postlesional, $p = 0.18$) or median MD ratio (1.06 prelesional vs 1.03 postlesional, $p = 0.9$). Analysis of the full lesion-containing fiber bundle similarly showed no change over time in median FA ratio (0.99 prelesional vs 0.89 postlesional, $p = 0.2$) or MD ratio (1.04 prelesional vs 1.03 postlesional, $p = 0.6$).

DISCUSSION The primary finding of this prospective longitudinal analysis is that small asymptomatic DWI hyperintense lesions are typically associated with microstructural alterations after a mean 7.1-month follow-up interval. These findings are consistent with the interpretation that these clinically silent, radiologically transient lesions represent small infarctions associated with persistent tissue damage. Because DTI abnormalities have been linked to cognitive performance,[22–25] these data suggest that the ongoing appearance of new lesions may contribute to vascular cognitive impairment in CAA.[26] We did not find evidence of acutely or chronically altered DTI parameters along white matter tracts outside of the lesion, however, suggesting that any effects at greater distances from the lesion are insufficient to be detected in the current small sample.

It is notable that these lesions produced chronic alterations in anisotropy and MD despite their very

Figure 3 Longitudinal changes of FA (A) and MD (B) ratios from pre- to postlesional scans

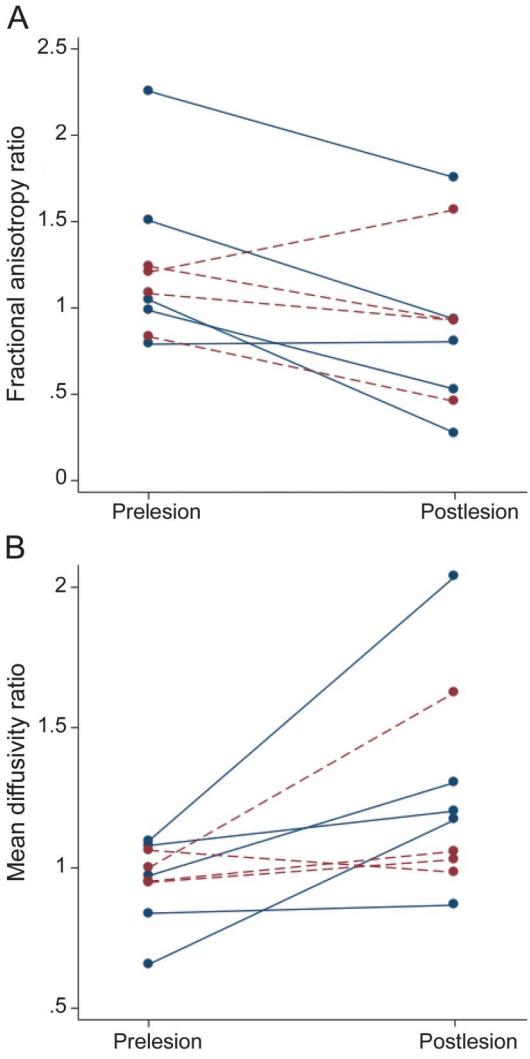

Dashed (red) lines represent the 4 lesions with no visible T1 or FLAIR changes at the lesion sites; solid (blue) lines the 5 lesions with visible T1 or FLAIR changes (see the results section). FA = fractional anisotropy; FLAIR = fluid-attenuated inversion recovery; MD = mean diffusivity.

small size and subtle structural imaging characteristics. Six of the 9 lesions were associated with either no detectable T1 or FLAIR changes (4 of 9) or with T1 hypointensities (2 of 9) below the 3- to 15-mm range used to define "lacunes of presumed vascular origin" in the recently proposed Standards for Reporting Vascular changes on Neuroimaging (STRIVE),[27] even when imaged at high resolution with precise localization to guide the reviewing investigators to the lesion sites. Indeed, even the 3 largest lesions were small enough (5–6 mm in largest diameter) to potentially evade detection without this type of high-resolution, spatially localizing information. The lesions were nonetheless disruptive enough of tissue microstructure to yield reduced FA and increased MD ratios of sufficient magnitude to reach statistical significance in this small dataset.

We did not find changes in FA or MD within the fiber tracts containing the lesions as have previously been identified in fiber tracts surrounding visible lacunar infarcts.[21] The absence of more widespread structural alterations suggests that the DWI lesions in the current study may be too small to produce measurable changes in downstream regions of white matter. An alternative explanation is that our method of normalizing all longitudinal DTI analyses to the contralateral control ROI to minimize interscan variability might bias toward a null finding, because the contralateral white matter tracts may also undergo progressive microstructural injury due to the effects of widespread CAA. Finally, our dataset of only 7 longitudinally imaged DWI lesions with tractography, although the largest reported to date, was underpowered for detecting modest effects. We note in this regard the nominally reduced FA ratio in the surrounding 6-mm fiber segments and the full lesion-containing fiber bundle ($p \leq 0.2$ for both comparisons), suggesting possible lesion effects to be looked for in larger future studies.

The strengths of our study are its prospective longitudinal design, the coregistration methods for localizing lesion and control ROIs on pre- and postlesional scans, and the use of high-resolution MRI scans obtained by research protocol rather than in response to any triggering clinical events. The study also benefited from the temporal information provided by DWI, allowing us to identify the timing of incident lesions. The main limitation was our small sample size noted above, a function of the relatively low frequency (approximately 10%–15%)[11–13] of DWI lesions even among subjects with advanced CAA. Interpretation of our data is also limited by the absence of neuropathologic correlation for the asymptomatic DWI lesions, another important goal for future studies.

The finding of altered DTI characteristics in association with small incident DWI lesions is consistent with the possibility that these lesions directly contribute to clinical conditions such as vascular cognitive impairment. Although the effect of an individual lesion (even one large enough to be detected by DWI) may be modest, the cumulative effect of an estimated hundreds or thousands of cerebral microinfarcts[2] distributed throughout the brain may be substantial. In the Adult Changes in Thought Study,[6] for example, CMIs were 1 of 3 independent neuropathologic predictors (along with Braak stage and neocortical Lewy bodies) for dementia, demonstrating an impressive 33% adjusted population attributable risk. Alterations in local and global brain network properties measured by MRI-based tractography have been found to correlate with information processing speed in type 2

diabetics[24] and mild cognitive impairment,[28] offering a potential mechanism by which small distributed lesions could generate cognitive impairments. The alterations in DTI parameters identified in the current study add a new link to the potential causal pathway between CMIs and neurologic dysfunction. They also serve to highlight the importance of ongoing studies to detect these tiny lesions and their impact on tissue structure in living patients.[7,8,29]

AUTHOR CONTRIBUTIONS

Study design: S.M.G., E.A., M.E.G. Data acquisition: E.A., P.F., A.K.R., A.V., S. R.-M. Data analysis: E.A., B.L.E., Y.D.R., M.E.G., S.M.G. Study management: S.M.G., K.S., A.V. Manuscript preparation: E.A., S.M.G., B.L.E. Manuscript review: all authors.

STUDY FUNDING

Supported in part by R01AG026484 and R25NS065743 from the NIH. The funding entities had no involvement in study design, data collection, analysis and interpretation, writing of the manuscript, or the decision to submit for publication.

DISCLOSURE

E. Auriel reports no disclosures relevant to the manuscript. B. Edlow: research support NIH (R25NS065743). Y. Reijmer, P. Fotiadis, S. Ramirez-Martinez, J. Ni, A. Reed, K. Schwab, and A. Vashkevich report no disclosures relevant to the manuscript. J. Rosand: research support NIH; consultant Boehringer Ingelheim; editorial advisory board memberships, *Lancet Neurology*, *Stroke*. A. Viswanathan: consultant Athena Diagnostics, data safety monitoring board Genentech, research support NIH (P50AG005134, K23AG028726). O. Wu: research support NIH (P50NS051343, R01NS59775) and Genentech, consultant Penumbra. M. Gurol reports no disclosures relevant to the manuscript. S. Greenberg: scientific advisory board/data safety monitoring board Hoffmann-La Roche, Quintiles; funding for travel/speaker honoraria New York Academy of Sciences, Quebec Society of Vascular Sciences, Cerebral Amyloid Angiopathy Conference, European Stroke Conference, American Academy of Neurology; editorial advisory board memberships, *Neurology*, *Stroke*, *Frontiers in Stroke*, *Cerebrovascular Disease*, *American Journal of Alzheimer's Disease & Other Dementias*; publishing royalties UpToDate, MedLink; research support NIH (R01AG026484, R01NS070834, U10NS077360). Go to Neurology.org for full disclosures.

Received December 20, 2013. Accepted in final form March 31, 2014.

REFERENCES

1. Smith EE, Schneider JA, Wardlaw JM, Greenberg SM. Cerebral microinfarcts: the invisible lesions. Lancet Neurol 2012;11:272–282.
2. Westover MB, Bianchi MT, Yang C, Schneider JA, Greenberg SM. Estimating cerebral microinfarct burden from autopsy samples. Neurology 2013;80:1365–1369.
3. Launer LJ, Hughes TM, White LR. Microinfarcts, brain atrophy, and cognitive function: the Honolulu Asia Aging Study Autopsy Study. Ann Neurol 2011;70:774–780.
4. Neuropathology Group. Medical Research Council Cognitive Function and Ageing Study. Pathological correlates of late-onset dementia in a multicentre, community-based population in England and Wales. Neuropathology Group of the Medical Research Council Cognitive Function and Ageing Study (MRC CFAS). Lancet 2001;357:169–175.
5. Arvanitakis Z, Leurgans SE, Barnes LL, Bennett DA, Schneider JA. Microinfarct pathology, dementia, and cognitive systems. Stroke 2011;42:722–727.
6. Sonnen JA, Larson EB, Crane PK, et al. Pathological correlates of dementia in a longitudinal, population-based sample of aging. Ann Neurol 2007;62:406–413.
7. Jouvent E, Poupon C, Gray F, et al. Intracortical infarcts in small vessel disease: a combined 7-T postmortem MRI and neuropathological case study in cerebral autosomal-dominant arteriopathy with subcortical infarcts and leukoencephalopathy. Stroke 2011;42:e27–e30.
8. van Veluw SJ, Zwanenburg JJ, Engelen-Lee J, et al. In vivo detection of cerebral cortical microinfarcts with high-resolution 7T MRI. J Cereb Blood Flow Metab 2013;33:322–329.
9. Burdette JH, Ricci PE, Petitti N, Elster AD. Cerebral infarction: time course of signal intensity changes on diffusion-weighted MR images. AJR Am J Roentgenol 1998;171:791–795.
10. Muir KW, Buchan A, von Kummer R, Rother J, Baron JC. Imaging of acute stroke. Lancet Neurol 2006;5:755–768.
11. Auriel E, Gurol ME, Ayres A, et al. Characteristic distributions of intracerebral hemorrhage-associated diffusion-weighted lesions. Neurology 2012;79:2335–2341.
12. Gregoire SM, Charidimou A, Gadapa N, et al. Acute ischaemic brain lesions in intracerebral haemorrhage: multicentre cross-sectional magnetic resonance imaging study. Brain 2011;134:2376–2386.
13. Kimberly WT, Gilson A, Rost NS, et al. Silent ischemic infarcts are associated with hemorrhage burden in cerebral amyloid angiopathy. Neurology 2009;72:1230–1235.
14. Basser PJ, Mattiello J, LeBihan D. MR diffusion tensor spectroscopy and imaging. Biophys J 1994;66:259–267.
15. Mori S, Crain BJ, Chacko VP, van Zijl PC. Three-dimensional tracking of axonal projections in the brain by magnetic resonance imaging. Ann Neurol 1999;45:265–269.
16. Gurol ME, Irizarry MC, Smith EE, et al. Plasma beta-amyloid and white matter lesions in AD, MCI, and cerebral amyloid angiopathy. Neurology 2006;66:23–29.
17. Knudsen KA, Rosand J, Karluk D, Greenberg SM. Clinical diagnosis of cerebral amyloid angiopathy: validation of the Boston Criteria. Neurology 2001;56:537–539.
18. Smith SM, Jenkinson M, Woolrich MW, et al. Advances in functional and structural MR image analysis and implementation as FSL. Neuroimage 2004;23(suppl 1):S208–S219.
19. Oishi K, Faria A, van Zijl PCM, Mori S. MRI Atlas of Human White Matter, 2nd ed. Amsterdam: Elsevier; 2011.
20. Tournier JD, Calamante F, Connelly A. Robust determination of the fibre orientation distribution in diffusion MRI: non-negativity constrained super-resolved spherical deconvolution. Neuroimage 2007;35:1459–1472.
21. Reijmer YD, Freeze WM, Leemans A, Biessels GJ. The effect of lacunar infarcts on white matter tract integrity. Stroke 2013;44:2019–2021.
22. Charlton RA, Barrick TR, McIntyre DJ, et al. White matter damage on diffusion tensor imaging correlates with age-related cognitive decline. Neurology 2006;66:217–222.
23. Viswanathan A, Patel P, Rahman R, et al. Tissue microstructural changes are independently associated with cognitive impairment in cerebral amyloid angiopathy. Stroke 2008;39:1988–1992.
24. Reijmer YD, Leemans A, Brundel M, Kappelle LJ, Biessels GJ. Disruption of the cerebral white matter network is related to slowing of information processing speed in patients with type 2 diabetes. Diabetes 2013;62:2112–2115.
25. Holtmannspotter M, Peters N, Opherk C, et al. Diffusion magnetic resonance histograms as a surrogate marker and

predictor of disease progression in CADASIL: a two-year follow-up study. Stroke 2005;36:2559–2565.
26. Arvanitakis Z, Leurgans SE, Wang Z, Wilson RS, Bennett DA, Schneider JA. Cerebral amyloid angiopathy pathology and cognitive domains in older persons. Ann Neurol 2011;69:320–327.
27. Wardlaw JM, Smith EE, Biessels GJ, et al. Neuroimaging standards for research into small vessel disease and its contribution to ageing and neurodegeneration. Lancet Neurol 2013;12:822–838.
28. Shu N, Liang Y, Li H, et al. Disrupted topological organization in white matter structural networks in amnestic mild cognitive impairment: relationship to subtype. Radiology 2012;265:518–527.
29. McNab JA, Edlow BL, Witzel T, et al. The human connectome project and beyond: initial applications of 300mT/m gradients. Neuroimage 2013;80:234–245.
30. Dick AS, Tremblay P. Beyond the arcuate fasciculus: consensus and controversy in the connectional anatomy of language. Brain 2012;135:3529–3550.